Available online at www.sciencedirect.com
ScienceDirect
Polymer 49 (2008) 934–942
polymer
www.elsevier.com/locate/polymer

The relationship between polyurethane foam microstructure and foam aging

Mark Sonnenschein [a,*], Benjamin L. Wendt [a], Alan K. Schrock [b], Jean-Marie Sonney [c], Anthony J. Ryan [d]

[a] Dow Chemical Company, Corporate Research and Development, Midland, MI 48640, United States
[b] Dow Chemical Company, Polyurethanes Research, Freeport, TX 77541, United States
[c] Dow Chemical Company, Polyurethanes Research, Freienbach 8807, Switzerland
[d] Department of Chemistry, University of Sheffield, Sheffield S3 7HF, UK

Received 24 October 2007; received in revised form 14 December 2007; accepted 5 January 2008
Available online 11 January 2008

Abstract

Correlations between polyurethane foam formulation and foam aging are shown to simplify when sufficient data are available to eliminate casual relationships. The numerous factors that are purported to result in faster or slower foam aging are shown to primarily reflect how those factors influence polyurethane hard segment structure. Specifically, changes in formulation that results in better phase separated (but co-continuous) structures exhibit less humid and heat aging than foams with poorer phase separation (broader interfacial phase mixing). This is demonstrated for aging tests that probe the polymer phase structure at higher stress or strain levels than that sometimes used. Tests that do not adequately stress the foam do not truly probe differences in foam structure that result in property decrements. Humid aged compression set and heat aged load loss data for a large number of foams are related to their formulation, catalysis, foaming rheology, and their hard segment structure determined by AFM and X-ray analyses.

Keywords: Polyurethanes; Foams; Structure–property relationships

1. Introduction

Flexible polyurethane foams are ubiquitous in our lives and have been studied in an amount almost proportional to their use [1–10]. In the mass of research there is a tremendous amount of work on foam fatigue properties. Fatigue, in its most generic definition, can be any decrement in foam performance as a function of aging. However, fatigue as a material property suffers from several confusions, one being that it is poorly defined by test methodology. Given the variety of tests, the same foam may exhibit very low fatigue in one venue and very high fatigue in another. For example, while two articles may purport to monitor the loss of foam load bearing capacity with age, one may age the foam under a constant load and the other may not, and so do not provide a common frame of reference. Furthermore, a laboratory may make a systematic change in foam formulation and observe a change in its measurement of fatigue. This casual relationship between dependent and independent variables may then be suggested as causative, when in fact there is an underlying cause that remains undetected. Modern techniques have improved this situation, but the number of reported causes for foam fatigue still remains discouragingly large [11–16].

In 1965 Kane [17] discussed different methods of measuring flexible polyurethane foam fatigue and several formulation factors that affect fatigue such as foam density and isocyanate index. Subsequently, Smith and Degisi [18] studied the effect of thermal aging on polyurethane foams as a function of hard segment structure and filler content. Campbell et al. [19]

* Corresponding author. The Dow Chemical Company, Corporate Research and Development, 1702 Building, Midland, MI 48674, United States. Tel.: +1 989 636 7415; fax: +1 989 636 4019.
E-mail address: mfsonnenschein@dow.com (M. Sonnenschein).

0032-3861/$ - see front matter © 2008 Elsevier Ltd. All rights reserved.
doi:10.1016/j.polymer.2008.01.008

looked at the effect of several formulation variables in humid aged compression set (HACS) and discussed the role of poorly networked urea oligomers on the measurement. Saotome et al. [20] discussed the relative fatigue properties of foams humid aged at different levels of strain and the effects of isocyanate index, soft segment molecular weight, and surfactant level. Herrington and Klarfeld [21] looked at the effect of hard segment volume, time and temperature on HACS. They observed that foams could recover a significant amount of their initial shape if provided sufficient time and in some cases temperature. Moreland and Wilkes [22] used numerous techniques to study the effect of strain on hard segment structure of flexible polyurethane foams. They observed strain-dependent disruption of the hard segment lamellae. Dounis et al. [23] studied the mechano-sorptive behavior of polyurethane foams. They found that periodic inhalation of moisture into foam under stress fatigued the foam to a greater extent than a steady exposure to moisture. Moreland et al. [24] studied stress relaxation of polyurethane foams as a function of temperature, humidity, density, and hard segment volume. They found that relaxation processes were independent of foam cell structure, and therefore are a fundamental property of the polymer making up the foam. Dounis and Wilkes [25] studied the structure–property relationships for fatigue of slab and molded flexible polyurethane foams, and found that hard segment structure was a critical aspect of compression set properties. They also correlated the use of diethanolamine (DEOA) in molded foams to poorer fatigue properties. Neff and Marsalko [26] studied the role of isocyanate and polyol structure on heat and HACS related fatigue. They observed that the hydrophilicity of the soft segment affected primarily the humid aged properties. However, these effects were reversible when moisture was removed from the polymer matrix. Sonnenschein et al. [27] showed that heat aged fatigue as measured by compression set was modulated by the presence of a third phase located at the hard/soft segment interface.

In this article we present results that show the independent factors that correlate to foam fatigue properties. Other factors are shown to have intermittent contribution to fatigue suggesting that the effects are really due to some other underlying factor. The true underlying factor can be masked by formulation or processing conditions. We show that for molded flexible polyurethane foams, hard segment structure, particularly the extent of phase separation, is the variable that consistently relates to heat aged and humid aged fatigue properties. Furthermore we show that factors appearing to have a direct influence on foam fatigue, might also be evaluated for their direct influence on hard segment structure.

2. Experimental

Bench scale molded foams were produced using a $30 \times 30 \times 10$ cm test mold heated to 60 °C using a standard hand mix procedure. Free-rise foams were poured into a 5 l plastic bucket. Machine-made foams were produced using high-pressure-impingment mixheads (Krauss–Maffei and Cannon) as standard test block molds ($40 \times 40 \times 10$ cm). Commercial polymeric MDI was used in these experiments including Specflex NE 150 and XNE 257.03 from Dow Chemical, Suprasec 2447 from Huntsman Chemical and Desmodur 3230 from Bayer Chemical Co. Each of these polymeric MDI samples has different, in some cases substantially different compositions. There is no attempt herein to identify individual data points with their corresponding raw material identities. Foam isocyanate index ([NCO]/[OH]) varied from 0.85 to 1.15, water levels varied from 3.1 to 4.4 parts per 100 parts polyol and numerous catalysts (reactive and conventional) and surfactants were employed based primarily on their ability to produce foam and not on their ability to produce a desired property result. Foam density was allowed to vary from 45 kg/m^3 to 131 kg/m^3. Polyol composition was only controlled to the extent that their part in the formulation resulted in representative foam samples. A list of the polyols and some of their relevant characteristics is given in Table 1.

While many fatigue properties were measured, only results for humid and dry aged load loss, and humid aged compression set for 50% and 75% compressions are reported. Some tests for load loss gave values that resulted in a small range. The greatest range was found in a test specified by Volkswagon (VW) which follows a procedure consisting of using samples $70 \times 70 \times 30$ mm initially equilibrated for 24 h at 23 °C and 50% relative humidity (ASTM standard). The foam sample is subsequently subjected to a 40% compression load deflection (CLD) test and that point is taken as the initial or unaged value of load bearing (CLD_o). In the CLD test the foam is compressed 4 times to 70% of its height. On the 4th cycle the measured load is recorded at 40% compression. Foam that has been tested but not aged is then placed in an environmentally controlled chamber (Russell Model # 3-300) for 200 h at 90 °C and 95% relative humidity. At the end of the aging procedure the foam is removed from the chamber and allowed to equilibrate at ASTM conditions for 24 h after which the 40% CLD is re-measured. The CLD change is calculated from the following equation.

Table 1
Relevant structural parameters on polyols used in this work

Polyol	Functionality	Equivalent weight	Comment
Voranol CP6001	3	2000	Glycerin initiated 15% EO capped
Voranol EP 2001	2	1000	Dipropylene glycol initiated 10% EO capped
Specflex NC 632	3.3	1750	Sorbitol/glycerin initiated 15% EO capped
Voranol CP 1421	3	1700	Glycerin initiated 75/25 EO/PO
Voranol Vorativ	4	1000	Bis(3-aminopropylamine)methyl amine initiated 15% EO capped
XNC 681.01	2	1000	*N*-Methyl diethanolamine initiated 15% EO capped
XZ 94864	4	900	Ethylene diamine initiated 15% EO capped
DEOA			85/15 (wt) blend of diethanolamine and water

$$\left(\frac{\mathrm{CLD}_{200}}{\mathrm{CLD}_0} - 1\right) \times 100 \quad (1)$$

CLD testing was performed on an Instron 5500 test frame using Merlin data collection software and a commercial spreadsheet program. Compression was achieved using a low mass aluminum honeycomb compression fixture connected to a 100 lb load cell.

Humid aged compression set (HACS) followed one of the industry standard test methods [21]. The test is conducted in two sequential steps. Foam samples ($10.2 \times 10.2 \times 2.5$ cm) are cut from the foam center and placed in a steam autoclave for 5 h at 121 °C at 100% relative humidity. The foam specimens are then placed in an oven at 70 °C at 50% humidity for 3 h to remove gross moisture. The compression set test begins by cutting $5 \times 5 \times 2.5$ cm specimens from the larger blocks, the height of the specimen is measured and then compressed to the desired amount (50% or 75%) of the original height. After 22 h in a 70 °C oven the samples are removed from the oven and allowed to equilibrate under no stress for 30 min under ASTM conditions. The recovered height is measured and the set is calculated by Eq. (2) where T_o is the initial thickness, T_f the final specimen thickness and T_s a correction for a spacer bar if used.

$$\%\mathrm{HACS} = \frac{(T_o - T_f)}{(T_o - T_s)} \times 100 \quad (2)$$

AFM data were obtained on a Digital Instruments Multimode using a Nanoscope IV controller. Silicon cantilevers and tips were used at a frequency of 158 kHz. The foam samples were prepared by initially embedding in epoxy and allowing to cure. The cured block was subsequently cryo-polished. The resulting face was exposed to RuO_4 vapor and then the block was re-polished at room temperature. Typical tapping conditions were $A_o \sim 1.0$ V, ASP ~ 0.6 V with the tip–surface interaction repulsive in nature.

Vibrating needle viscometry [28,29] was performed with a Rapra Technologies scanning needle viscometer. The viscometer was operated in a fixed frequency mode pre-set in air with a dwell time of 1 s. A 50 cm long 4 mm diameter carbon fiber rod was used for the needle.

Resilience [30] was determined by dropping a steel ball from a prescribed height and measuring the percentage of rebounded height.

Small angle X-ray scattering (SAXS) analyses for *d*-spacing were performed using the following procedure. Foam samples were cut to a width of 5 mm and placed in the Kratky camera under vacuum. The Kratky camera was aligned with a vertical X-ray tube stand where Cu K_{avg} radiation $\lambda = 1.54184$ Å was transmitted through the sample. SAXS from the sample traveled down the waveguide 72 cm where data were collected with a position sensitive detector. SAXS data were collected for 30 min through a q range from 0.01 $Å^{-1}$ to 0.138 $Å^{-1}$ which corresponds to *d*-spacings from 628 Å to 45.6 Å. SAXS data were analyzed using JADE XRD pattern processing software. Profile fit analyses were performed on the Intensity spectra and Lorentz (Iq^2) corrected data. Both methods yielded comparable trends with *d*-spacings from the Lorentz corrected data giving somewhat smaller absolute but generally more precisely determined values. Although the Lorentz correction is primarily reserved for lamellar crystalline structures, some have reported the polyurethane hard segment phase in flexible foams to be "lamellar like" [31,32] and this correction has been employed previously [27,33].

Small angle X-ray analysis was also performed at the European Synchrotron Research Facility in Grenoble, France [34]. Data were taken on the Dubble GRG station running at 10 KeV with $\lambda = 1.24$ Å, and a camera length of 2.5 m from sample position to detector. Two-dimensional SAXS collected each frame for 10 s corrected for sample thickness, non-linearity, and data distortion. An empty camera background was subtracted and the data averaged over a sector region into a 1-D plot. Calibration of the detector was accomplished with silver behenate ($d_{001} = 58.38$ Å). Full correlation function analysis was performed on the 1-D SAXS. A sigmoid tail model was applied in the analysis of the correlation function.

3. Results and discussion

In the past there was speculation that macroscopic features of foams such as air flow were directly related to foam fatigue [1,35]. However, it has since been recognized that the relevant length scale for understanding the material properties of polyurethane foams is of molecular dimensions. In fact, there are several studies suggesting that gross morphology can be essentially ignored in understanding PU foam properties [24,36]. This, however, may be an overstatement. It must be recognized that a foam's gross morphology is a reflection of the reactions and processes which result in the underlying polymer structure. With the very wide formulation range used for making foams, the processes responsible for foam structure and performance may overlay each other in unpredictable ways. For instance, there are several papers that report the influence of DEOA on foam properties and hard segment structure [31,37]. However, when a large number of foams with widely varying levels of DEOA are studied for effects on humid aged load loss (HALL) there is essentially no trend observed (Fig. 1). Given the wide variation of HALL at a single

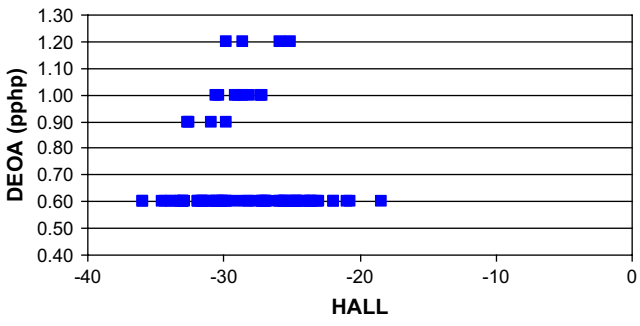

Fig. 1. Effect of diethanolamine addition on humid aged load loss.

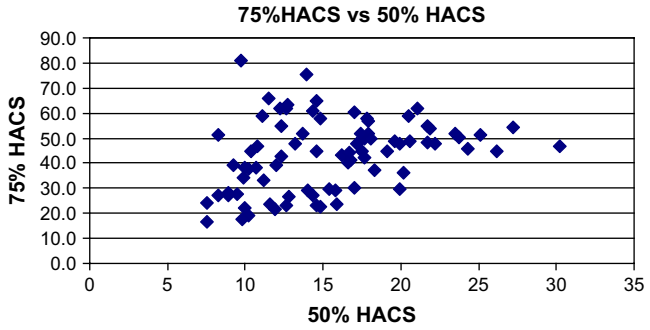

Fig. 2. Lack of relationship between humid aged compression set measured at 50% and 75% compression.

DEOA level and the number of similar HALL values at widely differing levels of DEOA, we demonstrate that HALL and DEOA are not directly linked. Instead HALL is related to some other factors with a casual link to DEOA level. This is not to say that formulation variables such as crosslinkers have no effect on foam structure. These effects are well documented. Instead this result suggests that DEOA does not dictate aging properties.

Surprisingly, even measurements of the same aging phenomenon but at different testing conditions can suggest almost no relationship. Fig. 2 demonstrates that an HACS measurement at 50% compression has virtually no relationship to the same measurement at 75% compression (N.B.: these measurements are on the same foam samples but not on the same test specimens). Again, it may be possible to control variables such that a given data set will suggest a relationship, but the phenomena related to one test cannot be confidently assessed to relate to others. To some extent this is a result of the relatively small range of values associated with 50% compression set test, which could with some confidence be assigned as $15 \pm 5\%$.

That seemingly related tests provide information on different foam characteristics can be demonstrated by observing the relationship between two low strain tests, 50% HACS and foam resiliency (Fig. 3). While the square of the correlation coefficient is hardly definitive, there is clearly a trend in the data. Unsurprisingly, there is no relationship between 75%

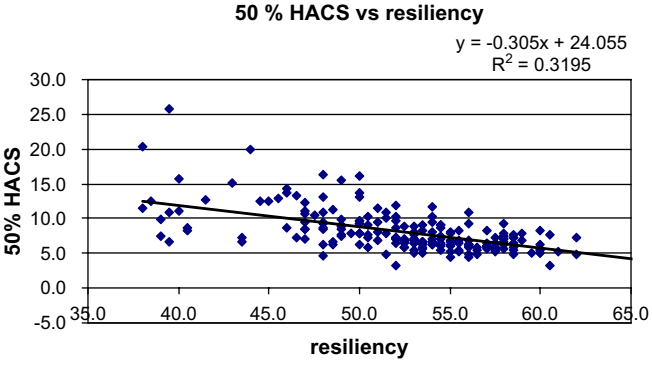

Fig. 3. Relationship between 50% humid aged compression set and resiliency measurements on molded polyurethane foams.

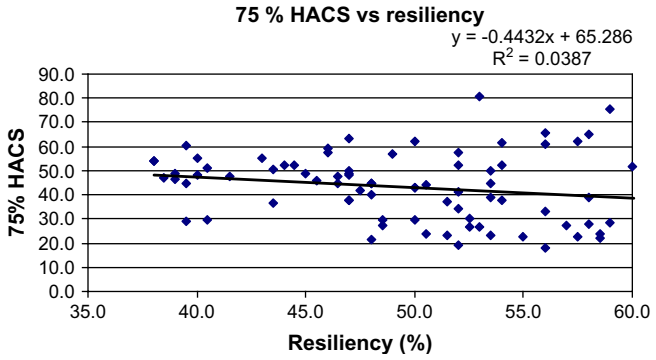

Fig. 4. Lack of relationship between 75% humid aged compression set and resiliency measured on molded polyurethane foams.

HACS (a high strain test) and resiliency (Fig. 4). Clearly, different foam structural characteristics are driving these properties.

We have observed that a reliable predictor of molded flexible foam aging is the hard segment *d*-spacing as determined by X-ray analysis. This is especially true for tests that yield a wider range of aging values as observed for HALL (Fig. 5). In the same regard we observe a close relationship between HALL (and therefore hard segment *d*-spacing) and 75% HACS but no such relationship to 50% HACS (Fig. 6). These results strongly suggest that hard segment structure, especially in connection to the extent of phase separation in the finished foam, is a structural feature that reliably influences the results of standard high strain aging tests. Since the majority of these foams does not vary widely in hard segment volume, the measurement of higher *d*-spacing is strongly related to phase separation and absolute hard segment thickness.

We can similarly investigate foam properties commonly associated with foam aging, such as foam hardness determined by a compressive force measured at 40% deflection (CFD

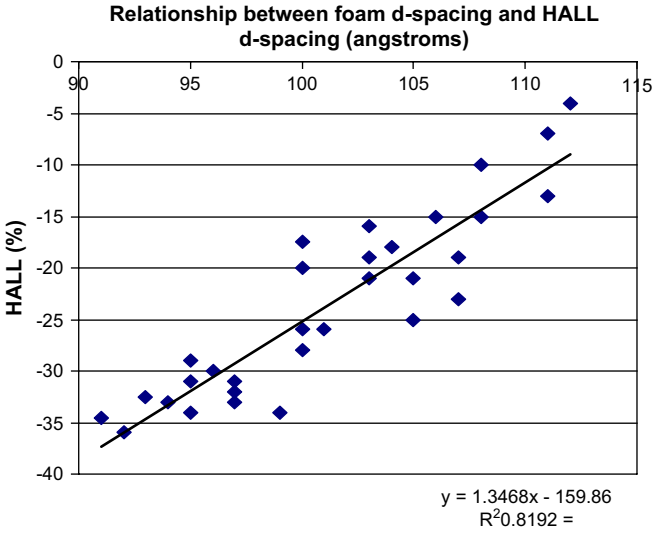

Fig. 5. Relationship between humid aged load loss and X-ray determined *d*-spacing.

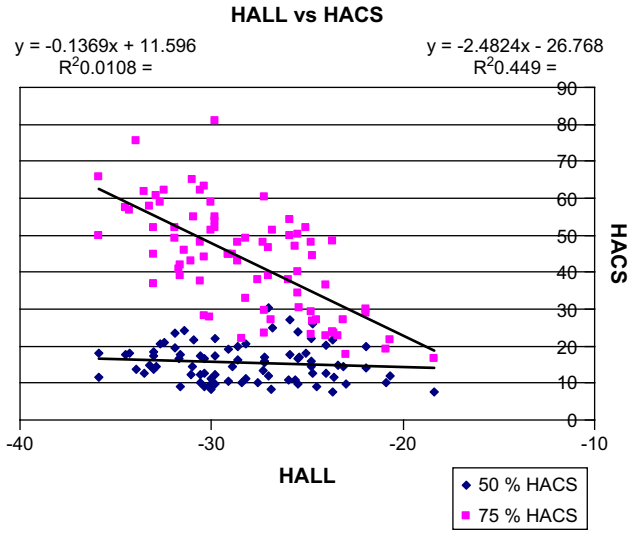

Fig. 6. Relationship between humid aged load loss and humid aged compression set at 50% and 75% compression.

40). To the extent the foam hardness is related to hard segment structure it might also be expected to correlate to foam aging measurements. However, because foam hardness may result from several structural features (such as intersegmental mixing [38]) that may have no relationship to well developed hard segment structure, or even are antagonistic to such structures, a poor relationship is observed (Fig. 7).

One structural parameter that intuition suggests should be strongly related to hard segment *d*-spacing and thus foam aging is the soft segment equivalent weight [39]. In keeping with intuition, the random phase approximation predicts that $q \times R_g \sim 2$ for a block co-polymer, where q is the SAXS peak position and R_g is the polymer radius of gyration which scales as $M^{2/3}$ [40]. This relationship has also been shown for a series of polyurethane materials [41,42]. Naturally, it is the soft segment length that puts initial boundaries on the distance between hard segments (but not the distribution of hard segment lengths or phase separation thermodynamics) and one would expect a significant correlation to this parameter. Fig. 8 shows that in fact such a correlation is observed, but it is not as strong as one might expect, simply because as parenthetically suggested, it is by itself not a deterministic parameter.

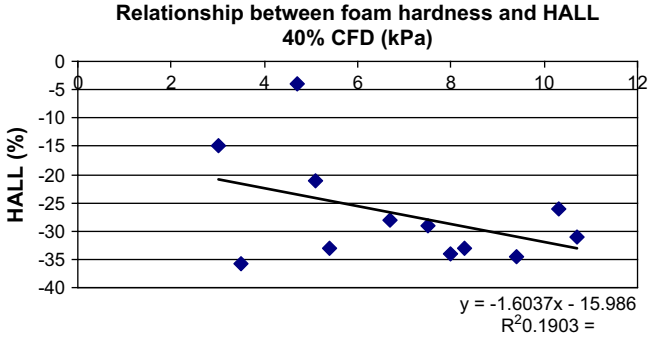

Fig. 7. Relationship between humid aged load loss and foam hardness.

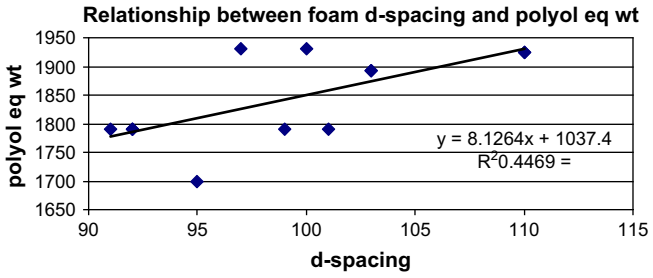

Fig. 8. Relationship between polyol equivalent weight and X-ray determined foam *d*-spacing.

Hard segment structural differences associated with molded polyurethane foams having different aging properties and different *d*-spacing values are visualized when they are imaged by atomic force microscopy (AFM) [43]. Representative images for a limited number of foams that were studied are presented in Fig. 9. One can see that foams with relatively low humid aged load loss possess a lacy percolating structure (Fig. 9a) that has previously been observed for these materials. The structure is consistent with the ~10 nm peak position seen in SAXS. Also, under close inspection one can observe crystalline fine structure. In contrast, foams with poorer aging properties typically possessed a more poorly defined hard segment structure with a droplet appearance (Fig. 9b). Also observed in this image is a large "urea ball". These structures are unconnected and do not contribute to *d*-spacing.

Additional data on hard segment structure can be obtained from a full analysis of the X-ray scattering. Representative SAXS patterns for two foams with widely varying HALL are shown in Fig. 10. It can be readily inferred from these two SAXS patterns, from the peak heights and widths, that the sample with low HALL has much better defined phase separation than the sample with high HALL. The corresponding correlation functions $\gamma_1(r)$ obtained using a Fortran implementation of the Strobl and Schneider algorithm given below

$$\gamma_1(r) = \frac{1}{Q}\int_0^\infty I(q)q^2\cos(qr)\mathrm{d}q \tag{3}$$

are shown in Fig. 11 and the derived data from the correlation functions are listed in Table 2.

As indicated, both of these materials have essentially the same hard segment content given by ϕ_H, but sample A has much thicker hard segment units (L_H) which are more uniform in shape (polydispersity) and have sharper interfaces (σ) [44].

That polymer structure is related to foam aging properties may upon reflection not be that surprising. That aging is so heavily related to a single parameter (hard segment phase separation) may be. The value of this knowledge is that it allows one to systematically change formulation in order to aim for new aging properties. Since so many formulation changes are possible it would be helpful to understand how polymer

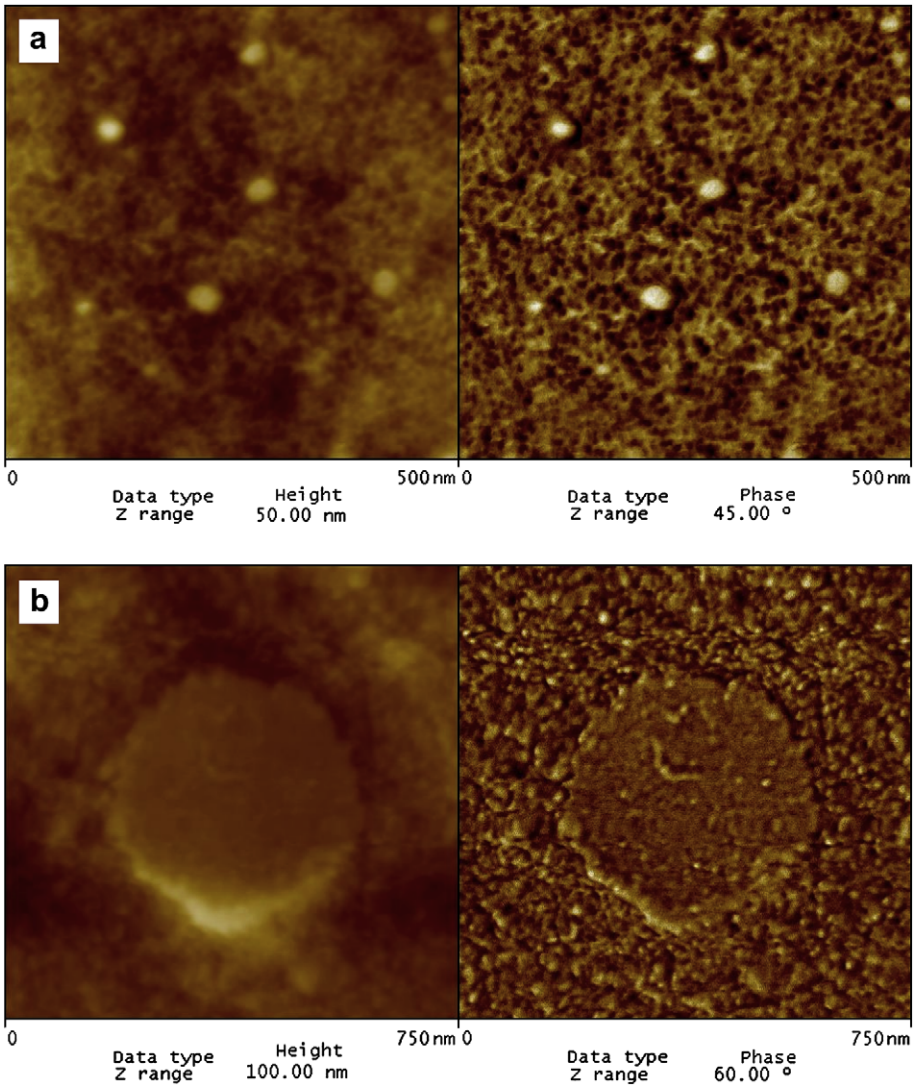

Fig. 9. AFM of foam samples with (a) very low (~5%) humid aged load loss and (b) relatively high (~35%) humid aged load loss. Left image is the height image and right is the phase image.

development during the foaming process relates to hard segment structure and ultimately to foam aging. In general, changes to formulation affect the competing reactions and processes related to urea formation (called the blowing reaction due to the formation of CO_2), phase separation of the hard segment blocks, and subsequent formation of urethane to form the gelled networked polymer (called the gelation reaction). Complications arise due to the simultaneous and therefore competitive nature of these reactions and the effect of formulation and process variability on the activation energy of these reactions. Direct measurement of foaming kinetics is notoriously difficult since the measurement can influence the process one is trying to measure [28,29]. One technique that has some applicability uses a vibrating needle rheometer. The specifics of the method can be found elsewhere [45,46]. In short, a vibrating needle is attached to a load cell measuring resistance to vibration as the foam rises. This resistance is observed as a load whose rheology can be back interpreted in terms of foaming reactions. Fig. 12 shows the frequency response of two representative foaming reactions. The increasing frequency is a direct measure of the growing viscosity of the foaming mass. Fig. 12a shows the data for a foam formulation resulting in foam with very small property loss after aging. Fig. 12b shows the data obtained on a foam formulation found to yield foams with poor aging.

It was found consistently that foams with good aging properties show an initial increase in frequency (a proxy for viscosity) associated with phase separation of the hard segment from the rest of the foaming mass. There may be subsequently an inflection where the isocyanate water reaction has largely been exhausted, but the gelation reaction is not occurring as fast as it subsequently does after about 170 s. Fig. 12b exhibits qualitative and quantitative differences with Fig. 12a. In the present case the slope from 100 s to 160 s in Fig. 12b is 42% less than the slope from 110 s to 130 s in Fig. 12a. The slow initial reactions described in Fig. 12b result in gelation accelerating before the isocyanate water reaction had been exhausted. Thus the gelation of the foam structure in

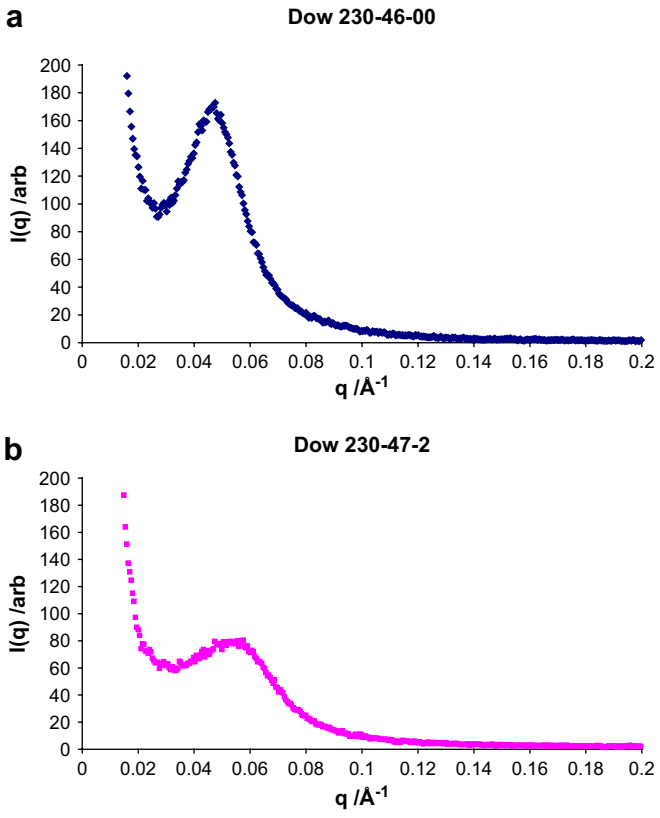

Fig. 10. Small angle X-ray scattering of molded polyurethane foams with (a) low (~5%) humid aged load loss and (b) relatively high (~35%) humid aged load loss. Both foams have the same hard segment volume, but B has a different polyol composition than A.

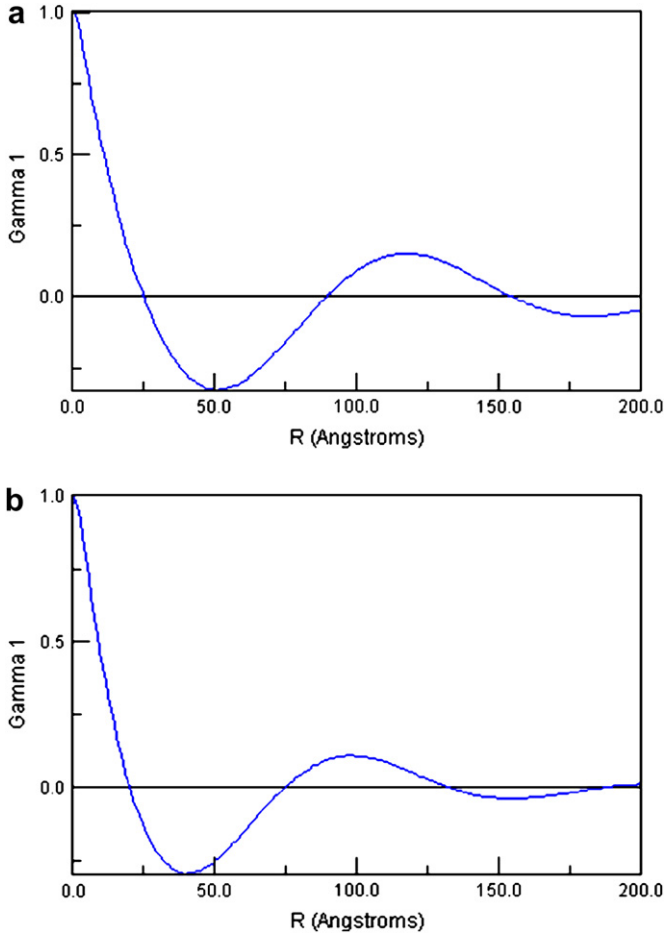

Fig. 11. Correlation functions for the corresponding scattering data in Fig. 10.

Table 2
Porod analysis of the correlation functions in Fig. 11

	Sample A	Sample B
HALL (%)	5	35
d-Spacing (Å)	118	98
L_H, hard block thickness (Å)	26.3	20.9
L_S, soft block thickness (Å)	91	77.0
ϕ_v, bulk volume crystallinity	0.23	0.21
ϕ_H, local crystallinity	0.22	0.21
σ interface thickness (Å)	3.0	4.0
Polydispersity	0.23	0.37

Fig. 12b is increasing the rate before the phase separation of the hard phase is complete and the system becomes vitrified in a less organized block co-polymer structure. It should be emphasized that the differences described may be subtle. Foams that age differently may appear quite similar prior to aging and only are differentiated when placed in extreme circumstances.

The indirect connection between foam aging and polymerization kinetics is further validated by determining the effect of foam catalysis on foam aging. In this way we do not see the effect of a foam formulation component, but rather a variable that indirectly influences the structure of the foam by changing the relative blow and gel reaction rates. Fig. 13 shows the statistical relationship between the amount of gelation (in this case triethylene diamine – TEDA) and the blowing catalyst (in this case bis(dimethylaminoethyl)-ether – DMAEE) on the subsequently measured humid aged load loss.

Fig. 13 shows that humid aged load loss is decreased when either the blowing or gelation catalyst is increased. The correlation in these plots is far from perfect, but the relationships illustrate the effect of catalysis on HALL independent of any other formulation or process change. The correlation is suggestive of the importance of catalysis on hard segment structuring. The importance of catalysis upon development of the hard segment structure is also highlighted by the greater slope for blowing reaction catalysis (urea producing) than that for the gelation reaction (urethane producing). That TEDA is positively correlated with decreased aging points to the fact that although it is primarily a gelation catalyst, TEDA does promote urea formation as well. We have found (data not shown) that TEDA not only has a strong gelation component, but also has a high activation energy and a threshold temperature below which it is more effective at the blowing reaction and less effective at the gelation reaction.

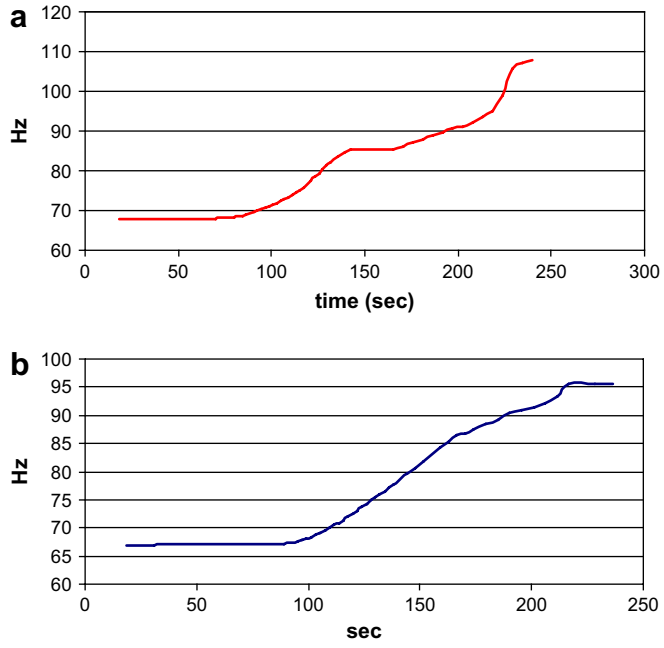

Fig. 12. Time-resolved vibrating needle rheometry of polyurethane foam formulations that result in (a) foams with very low aging and (b) relatively high foam aging.

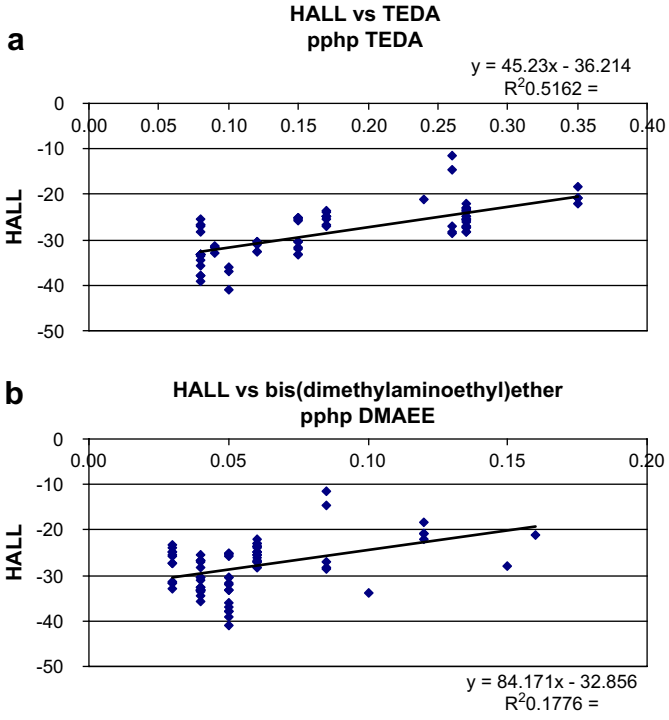

Fig. 13. Relationship between humid aged load loss and amount of (a) catalyst added for the purpose of speeding up gelation and (b) catalyst added for the purpose of speeding up the formation of urea (the blow reaction) to foaming mixtures.

4. Conclusion

Aging properties of polyurethane foams are shown to correlate most strongly with the X-ray determined hard segment *d*-spacing and other parameters associated with more complete hard segment phase separation. Formulation variables are shown to relate to aging only as they affect the hard segment structure. Furthermore, formulation variables that strongly affect hard segment structure may not strongly affect foam aging if the aging test itself does not adequately probe hard segment structure. In such a case all of the foam aging values will be clustered around some mean value. Such clusters may or may not give the impression of a relationship between independent and dependent variables, but will in fact not be probing the relevant structural variables.

References

[1] Herrington R, Hock K, editors. Dow polyurethanes flexible foams. 2nd ed. Midland, MI: Dow Chemical Publications; 1997.
[2] Elwell MJ, Ryan AJ, Grunbauer HJM, Van Lieshout HC. Macromolecules 1996;29:2960–8.
[3] Aneja A, Wilkes GL. J Appl Polym Sci 2002;85:2956–67.
[4] Zhang XD, Neff RA, Macosko CW. In: Lee ST, Ramesh NS, editors. Polymeric foam: mechanisms and materials. Boca Raton, FL: CRC Press; 2004. p. 139–71 [chapter 5].
[5] Pollack SK, Shen DY, Hsu SL, Wang Q, Stidham HD. Macromolecules 1989;22:551–7.
[6] Sonnenschein MF, Lysenko Z, Brune DA, Wendt BL, Schrock AK. Polymer 2005;46:10158–66.
[7] Bras W, Derbyshire GE, Bogg D, Cooke J, Elwell MJ, Komanschek BU, et al. Science 1995;267:996–9.
[8] Martin C, Eeckhaut G, Mahenrasingam A, Blundell DJ, Fuller W, Oldman RJ, et al. J Synchrotron Radiat 2000;7:245–50.
[9] Szayna M, Voekel R. Solid State Nucl Magn Reson 1999;15:99–102.
[10] Elwell MJ, Mortimer S, Ryan AJ. Macromolecules 1994;27:5428–39.
[11] Martin DJ, Meijs GF, Renwick GM, McCarthy SJ, Gunatillake PA. J Appl Polym Sci 1996;62:1377–86.
[12] Kaushiva BD, McCartney SR, Rossmy GR, Wilkes GL. Polymer 2000; 41:285–310.
[13] Beck RA, Truss RW. J Appl Polym Sci 1999;71:959–66.
[14] Yoon PJ, Han CD. Macromolecules 2000;33:2171–83.
[15] Nichetti D, Cossar S, Grizzuti N. J Rheol 2005;49:1361–76.
[16] Fishback T, Aviles G, Reichel C. Adhes Age 1996:20–3.
[17] Kane RP. J Cell Plast 1965;2:217–22.
[18] Smith CH, Degisi SL. J Appl Polym Sci 1966;10:795–805.
[19] Campbell GA, Dearlove TJ, Meluch WC. J Cell Plast 1976;12:222–6.
[20] Saotome K, Matsurbara K, Yatomi T. J Cell Plast 1977;13:203–9.
[21] Herrington RM, Klarfeld DL. J Cell Plast 1984;20:58–63.
[22] Moreland JC, Wilkes GL. J Appl Polym Sci 1991;43:801–15.
[23] Dounis DV, Moreland JC, Wilkes GL, Dillard DA, Turner RB. J Appl Polym Sci 1993;50:293–301.
[24] Moreland JC, Wilkes GL, Turner RB. J Appl Polym Sci 1994;52: 549–68.
[25] Dounis DV, Wilkes GL. Polymer 1997;38:2819–28.
[26] Neff RA, Marsalko TM. J Cell Plast 1999;35:492–513.
[27] Sonnenschein MF, Prange R, Schrock AK. Polymer 2007;48:616–23.
[28] Zhang XD, Giles DW, Barocas VH, Yasunaga K, Macosko CW. J Rheol 1998;42:871–89.
[29] Singh AP, Bhattacharya M. Polym Eng Sci 2004;44:1977–86.
[30] Standard test methods for flexible cellular materials. Philadelphia: American Society for Testing and Materials; 2005. D3574-05.
[31] Li W, Ryan AJ, Meier IK. Macromolecules 2002;35:6306–12.
[32] Koberstein JT, Galambos AF, Leung LM. Macromolecules 1992; 25:6195–204.
[33] Ophir Z, Wilkes GL. J Polym Sci Polym Phys Ed 1980;18:1469–80.
[34] Bras W, Dolbnya IP, Detollenaere D, van Tol R, Malfoi M, Greaves GN, et al. J Appl Crystallogr 2003;36:791–4.
[35] Skorpenske RG, Solis R, Kulies RA, Schrock AK, Turner RB. Proc SPI Annu Tech Mark Conf 1992;34:650–9.

[36] Armistead JP, Wilkes GL, Turner RB. J Appl Polym Sci 1988;35:601–29.
[37] Kaushiva BD, Wilkes GL. Polymer 2000;41:6981–6.
[38] Van der Schuur M, van der Heide E, Feijen J, Gaymans RJ. Polymer 2004;45:2721–7.
[39] Harrell LL. Macromolecules 1969;6:607–12.
[40] Leibler L. Macromolecules 1980;13:1602–17.
[41] Wilkinson AN, Naylor S, Elwell MJ, Draper P, Komanschek U, Stanford JL, et al. Polymer 1996;37:2021–4.
[42] Wilkinson AN, Elwell MJ, Ryan AJ. Polymer 2000;41:2569–76.
[43] Garrett JT, Siedlecki CA, Runt J. Macromolecules 2001;34:7066–70.
[44] Ryan AJ, Stanford JL, Bras W, Nye TMW. Polymer 1997;38:759–68.
[45] McClusky JV, O'Neil RE, Priester RD, Ramsey WA. J Cell Plast 1994;30:224–41.
[46] Schram LL. Colloid rheology. In: Schram LL, editor. Emulsions foams and suspensions. Munich: Wiley-VCH Verlag; 2006 [chapter 6].